ELSEVIER

Microstructure and Nanochemistry of Carbide Precipitates in High-Speed Steel S 6-5-2-5

Eckhard Pippel,* Jörg Woltersdorf,* Gottfried Pöckl,† and Gerhard Lichtenegger†

**Max-Planck-Institut für Mikrostrukturphysik, Weinberg 2, D-06120 Halle, Germany; and*
†Böhler Edelstahl GmbH, P.O.B. 96, A-8605 Kapfenberg, Austria

Depending on the steel composition several types of carbides are precipitated in high-speed steels: mainly MC, M_2C, M_6C and some others with minor importance. During hot working, the primary carbides formed during solidification change their as-cast structure to a more spherical one. They have an incoherent interface to the matrix and are a few micrometers in size. In the finished tool, the primary carbides together with the secondary, and the high hardness of the matrix are responsible for the high wear resistance. For the production of tools it is necessary that the steels can be machined, which is enabled by soft annealing. During this heat treatment some additional carbides of 50 to 300nm in size are precipitated as demonstrated by high-voltage electron microscopy (HVEM). After machining, the tools get their desired properties from hardening and tempering. The examination under these conditions shows the existence of nanometer-sized secondary hardening carbides, precipitated during this heat treatment and consisting mainly of vanadium and carbon as proven by energy filtered transmission electron microscopy (EFTEM). The high red hardness up to temperatures of approximately 550°C is caused by these nanometer-sized carbides. High resolution electron microscopy (HREM) revealed a completely coherent transition of the lattice planes from these carbides to the matrix-, without any irregularities.

INTRODUCTION

High-speed steels are highly alloyed, ledeburitic iron alloys. In use, the special features of these steels are: high hardness, strength and red hardness, combined with a correspondingly high toughness. These excellent properties result from a well-defined balance of the alloying elements carbon, chromium, tungsten, molybdenum, vanadium, and cobalt [1–4].

The production of high speed steel starts with the melting of pre-alloyed scrap and additions in an electric arc furnace. In these days the electric arc furnace is mainly a melting furnace. The treatment of the melt is carried out in the secondary metallurgical ladle treatment. The alloying constituents are adjusted in a very narrow range and the melts are deoxidized. The stirring of the melt with inert gas, i.e., nitrogen or argon, assists the removal of the primary non-metallic inclusions. The temperature is set in the ladle furnace and the melt is cast in ingots or in the continuous casting machine. Whereas in the continuous casting process additional cooling with a mixture of water and gas is applied, no such cooling is sufficient in ingot casting. The cooling system in the continuous casting process increases the solidification rate and refines the microstructure of the material.

The solidified ingots are heated up in furnaces to hot forming temperatures and depending on the sizes and the grades are hot forged in the long forging machine or

MATERIALS CHARACTERIZATION 43:41–55 (1999)

655 Avenue of the Americas, New York, NY 10010
1044-5803/99/$–see front matter
PII S1044-5803(99)00003-0

rolled in the blooming mill down to a cross section around 100mm in square. Further down, the billets are hot formed in a continuous process to the final dimensions in a multiline rolling mill. After hot rolling an annealing process is carried out in an annealing furnace which makes the material soft enough for machining.

The material is used by tool makers to produce twist drills, tops, milling cutters, reamers, saws etc. In the soft annealed condition the material is machined to the final shape.

By the following heat treatment, that is, hardening and tempering, the properties of the material are adjusted to the specific application. Sometimes the heat treatment is done by the toolmakers, often it is performed in well-equipped commercial heat treatment centers [5]. Over the past decade, hardening in vacuum furnaces has replaced the hardening in salt baths [6].

In a vacuum furnace the machined tools are heated-up in vacuum at a pressure below 1mbar. This kind of heating relies upon radiation for heat transfer. Such furnaces are most efficient and more readily achieve thermal uniformity at higher temperatures, but there is relatively little radiation heat at lower temperatures. In this range it is most efficient to use re-circulated inert gas as a means of heat transfer. Where a furnace has a convection-assisted heating facility, it is normal practice to heat the load to about 700°C in re-circulated nitrogen prior to pumping a vacuum and so reducing the heat-up time.

Quench rates are very important if the optimum properties are to be achieved from high speed steel. It is necessary to cool the work at such a speed that the proeutectoid and pearlite precipitation zones are avoided and the maximum volume of alloying elements is retained in solution in the matrix [7]. Fast cooling is nowadays achieved in vacuum furnaces by gas quenching with nitrogen. In the future, the competition by other quenching media will be strong with a new competition arising, e.g., mixtures of air and liquid media, the so called dual phase quenching media [7]. Figure 1 illustrates the production route of high-speed steels.

In the following, we present results on the microstructure and nanochemistry of an S 6-5-2-5 steel with a qualitative description of the distribution and composition of nanometer-sized carbide precipitates. The knowledge of these features can be used for micromechanical finite element (FEM) calculations, leading to a better understanding of the structure/property relations [8, 9], and to improvements of the microstructure.

Such calculations are based on a three-level hierarchical model, which is working on a macro-, meso-, and micro-level. The macro-level characterizes the geometry and the stress distribution in a tool. The meso-level is related to the cluster topology of carbide-rich areas and their distribution in the steel, whereas the micro-level describes the inner structure of the mesophases, i.e., the interaction between the carbides and the matrix.

Thin foils of high-speed steels have been investigated down to atomic dimensions using high voltage (HVEM) and high resolution electron microscopy (HREM), including energy filtered transmission electron microscopy (EFTEM). The latter enables the imaging with inelastically scattered electrons of a certain energy range. The combination with appropriate computer equipment enables the sensitive mapping of a specific element with a high spatial resolution (about 2nm) within a few seconds.

EXPERIMENTAL

High-speed steel S 6-5-2-5 is a complex alloyed material consisting of 0.92% C, 0.42% Si, 0.27% Mn, 0.027% P, 3.93% Cr, 6.12% W, 4.77% Mo, 0.39% Ni, 1.74% V, 0.17% Cu, 4.59% Co, 0.018% Al, 0.018% N. During annealing and tempering, especially V, Mo, W, and Cr form a number of carbides of different size and composition, which strongly influences the toughness and strength of the resulting steel as described in more detail in section 3. The investigated steel samples were cast as slightly conical ingots with the approximate dimensions of 300 × 300mm in

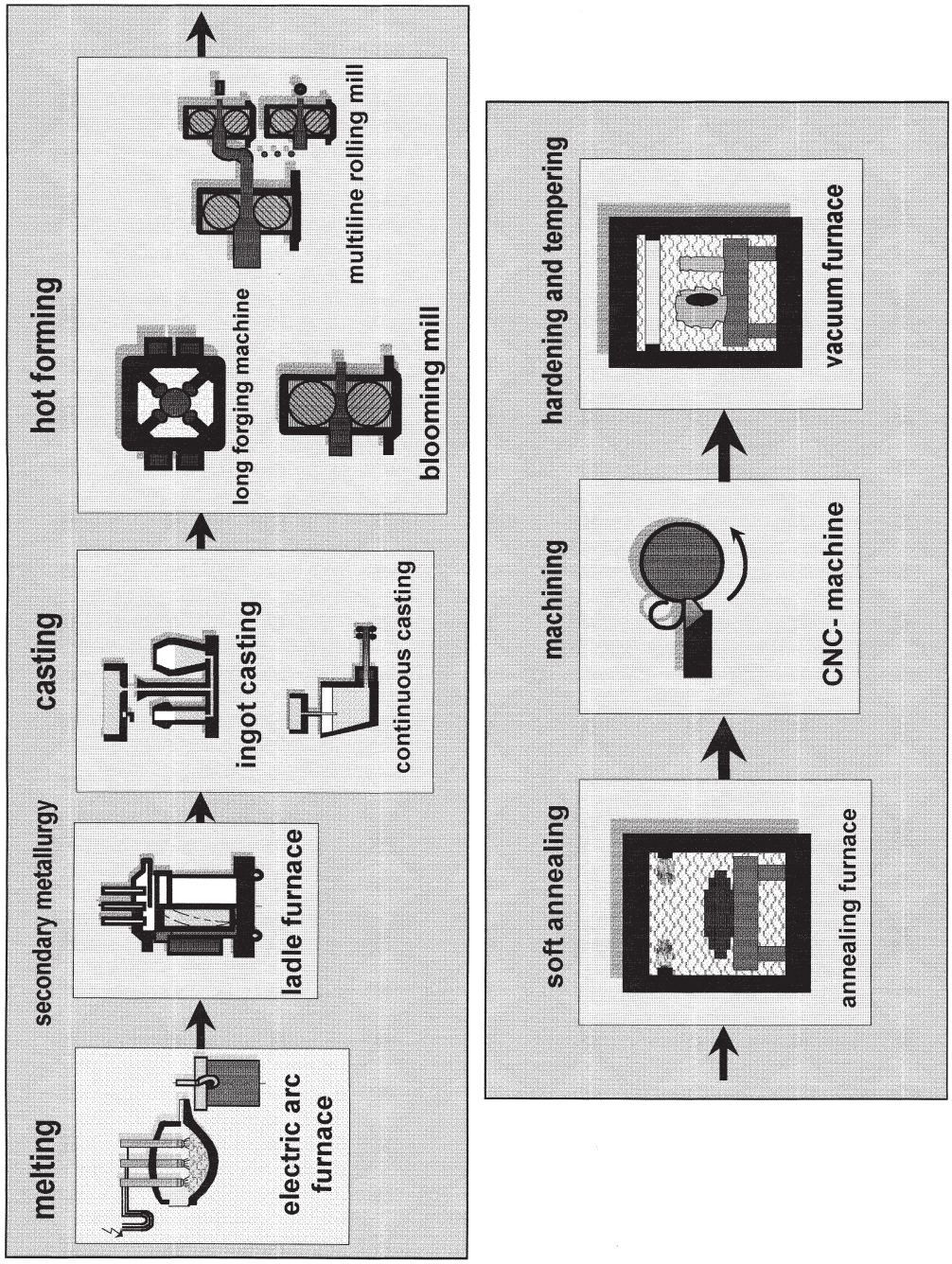

FIG. 1. Production route of tools made of high-speed steels (schematic).

the sectional area. The ingots were hot formed in two heats down to 12.2 mm in diameter. The investigation was performed on material in two different fabrication stages: (i) after annealing, and (ii) after hardening and tempering.

For electron microscope investigations, thin specimens were prepared by standard techniques, i.e., cutting thin (<200μm) slices, dimple-grinding to about 10 μm, and finally Ar-ion milling down to electron transparency. This provides specimens for high resolution and energy filtered imaging of only a few nanometers in thickness and a tolerable surface roughness.

Microstructure investigations followed using a high voltage electron microscope Jeol-JEM 1000-06 run at 1000kV, and a high resolution Philips CM 20 FEG field emission electron microscope, run at 200kV. The latter was equipped with a Gatan Imaging Filter (GIF 200), mounted below the microscope column. Besides electron energy loss spectroscopy (EELS), this filter enables element or chemical-bond specific imaging (EFTEM). Filtered images and some TEM bright-field images were digitally recorded by a slow-scan CCD camera within the GIF. Further details concerning the proper operation conditions of the GIF equipment are given in [10]. For image processing and EEL spectrum treatment the Gatan Digital Micrograph and ELP software, resp., loaded on a Power Macintosh 7200/75, were employed.

Contrary to the carbide extraction from the steel, which allows a phase determination by diffraction methods and x-ray spectroscopy [11], our foil preparation technique preserves the exact three dimensional distribution of the carbides and their interface to the matrix.

MICROSTRUCTURE OF HIGH-SPEED STEELS

STRUCTURE DEVELOPMENT DURING THE PRODUCTION PROCESS

The achievable properties strongly depend on the microstructure. In the solidified ingot of a S 6-5-2-6 steel the iron dendrites are surrounded by a carbide network. The solidification starts at about 1400°C with the formation of low-alloyed bcc δ-Fe. The remaining melt is enriched with the alloying elements, C, W, Mo, V, Cr, and Co. Therefore, 70–100°C below the above temperature, the peritectic reaction starts, during which δ-Fe, already formed, together with the melt transforms into γ-Fe. DTA-measurements often show a strong undercooling of this reaction. Nevertheless, the peritectic reaction always starts before the eutectic growth of the carbides. The eutectic temperature is as high as 1250°C. In the complex alloyed high-speed steel S 6-5-2-5, three types of primary carbides may form: fcc MC, hcp M_2C, or fcc M_6C-carbides (M-metal), of a few micrometers in size. The type of the growing carbides depends on the fine adjustment of the melt, the enrichment of the alloying elements and the solidification rate [4, 12, 13].

The elements V, C, and N promote the formation of MC-carbides. More than 1% of V is needed to form MC-carbides in high-speed steels. Other MC-forming elements are Ti and Nb, which are rarely used for producing conventional high-speed steels. M_2C-carbides are favored by the presence of Mo, while W and Si encourage the formation of M_6C. MC and M_6C are thermodynamically stable carbides whereas M_2C is metastable and immediately formed upon quick solidification. On slow cooling, the more stable M_6C carbide is forming, though owing to its complicated structure, it is growing more slowly [14–16].

Figure 2 shows the as-cast structure of a high-speed steel solidified by M_2C-carbides. The dark areas are the iron dendrites precipitated directly from the melt. The carbides appear as white phases within the interdendritic areas.

During annealing at higher temperatures for several hours the M_2C-carbides decompose by the following reaction [17]:

$$M_2C + y \rightarrow M_6C + MC + \alpha + C_\gamma$$

The metasabile M_2C phase reacts with the austenitic matrix and forms the carbides of the type M_6C and MC. Addition-

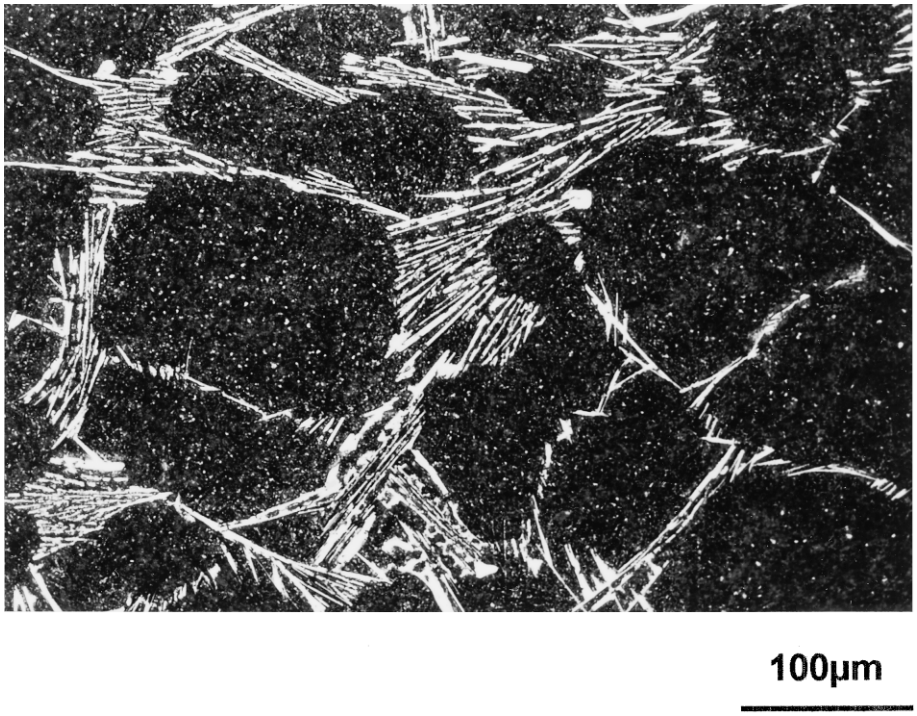

FIG. 2. As-cast microstructure of high-speed steel S 6-5-2 (optical microscopy).

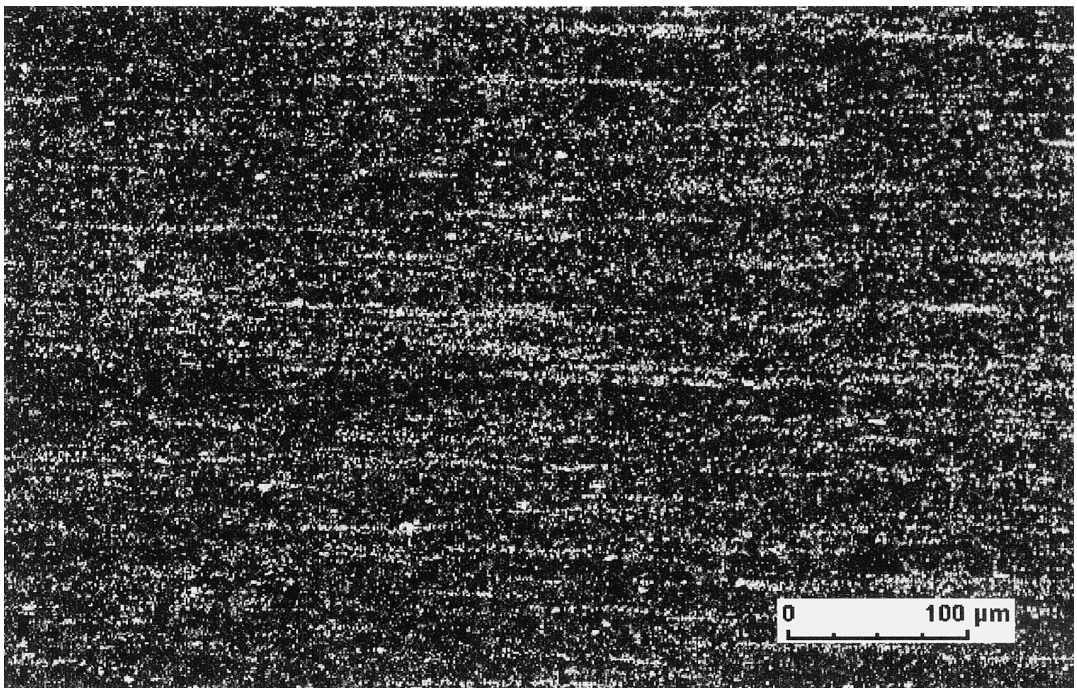

FIG. 3. Microstructure of the hot-deformed high-speed steel (optical microscopy).

ally in S 6-5-2 during this reaction, ferrite with a high content of W, Mo, and V is formed and there is a flow of carbon from the M_2C into the austenite.

Moreover, the microstructure changes during hot and cold forming. The carbides of the high-speed steels are arranged within the so-called carbide stringers.

Figure 3 shows the typical micrograph of a longitudinal metallographic specimen of the high-speed steel bar with a diameter of 12.2mm.

Depending on the reduction rate deformed carbide networks or carbide stringers occur. In small dimensioned steels with a high reduction rate only isolated carbides exist. Besides, the thermal and mechanical treatments during hot forming change the morphology of the carbides, i.e., rounding the edges and spheroidizing the carbides to minimize the surface energy.

STRUCTURE AFTER ANNEALING

Annealing is used to reduce the hardness of the material to enhance the machinability of high-speed steels. Temperatures are applied far below the hot forming temperature. During annealing the iron matrix reduces its alloying content, with annealing carbides forming. After soft annealing, high-speed steels contain a ferritic matrix with primary and annealing carbides [1].

Figure 4 shows a HVEM image of the microstructure of an annealed steel at medium magnification. In the middle, there is a primary carbide grain of about 2μm in diameter. The smaller dark-contrasted particles between 50nm and 300nm in diameter are the carbides resulting from the annealing procedure. Furthermore, the large number of dislocations in the ferritic matrix indicates strong residual plastic deformations in the material.

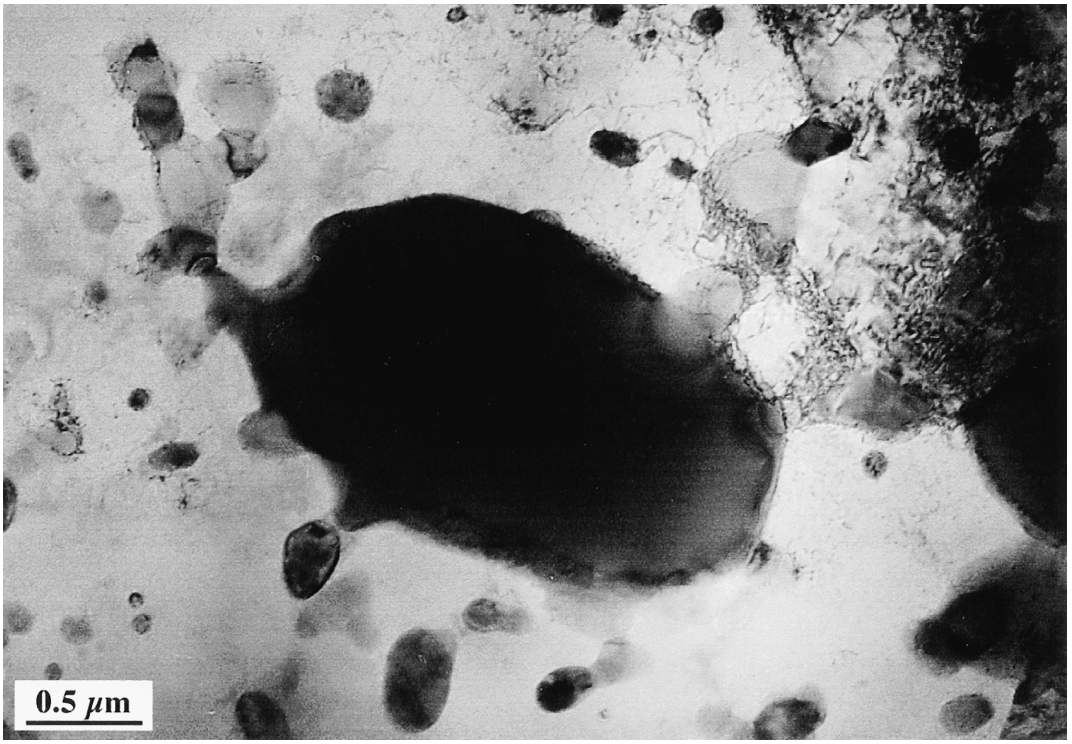

FIG. 4. Microstructure of the annealed steel (HVEM).

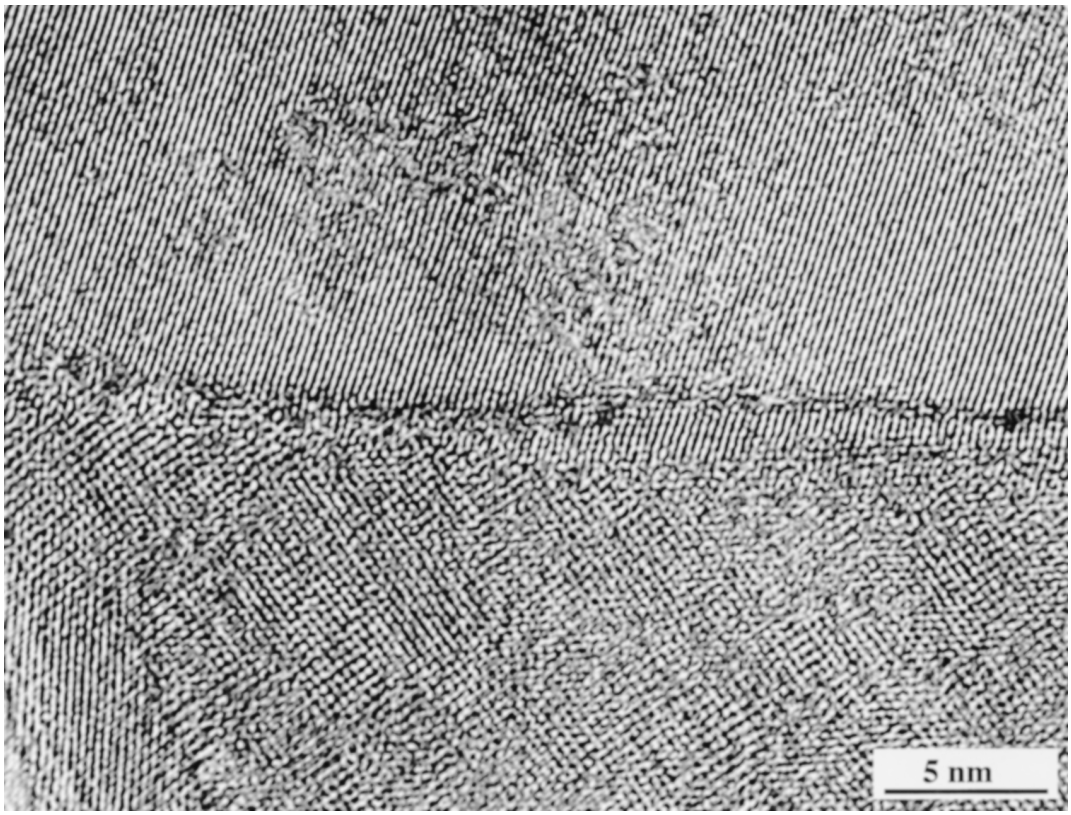

FIG. 5. HREM image of the interface of a primary carbide (above) and the ferritic matrix (below).

The interface between a primary carbide grain and the matrix is shown in the atomic lattice resolution image of Fig. 5. This interface seems to be free of other crystalline phases. Because of the complicated image formation conditions (both adjacent crystals have to fulfil the Bragg diffraction condition, and the interface has to be in parallel orientation to the electron beam) the existence of a 1–2-nm thin amorphous interlayer cannot be excluded, however.

STRUCTURE AFTER HARDENING AND TEMPERING

High-speed steel tools get their final shape by machining. The properties desired are achieved by a special heat treatment in two steps: hardening and tempering. Figure 6 presents a time-temperature curve.

The different parameters, i.e., hardening temperature, soaking time, tempering temperature, number of tempering steps, etc., are adapted to the application of the tool. Hardening should immediately be followed by tempering at 540–560°C. The complete transformation of the remaining austenite into martensite and a homogeneous microstructure require tempering at least two or three times.

The typical microstructure of the material hardened at 1200°C and tempered three times at 560°C for one hour is shown in the HVEM image of Fig. 7. Because of the fine martensitic structure of the matrix (plates, needles) there is almost no mesoscopic grain structure. Within the matrix there are again round primary carbides of some micrometers in diameter (dark contrast) clearly showing contours of mechanical strain.

At higher magnification (see Fig. 8), the matrix reveals a large number of almost

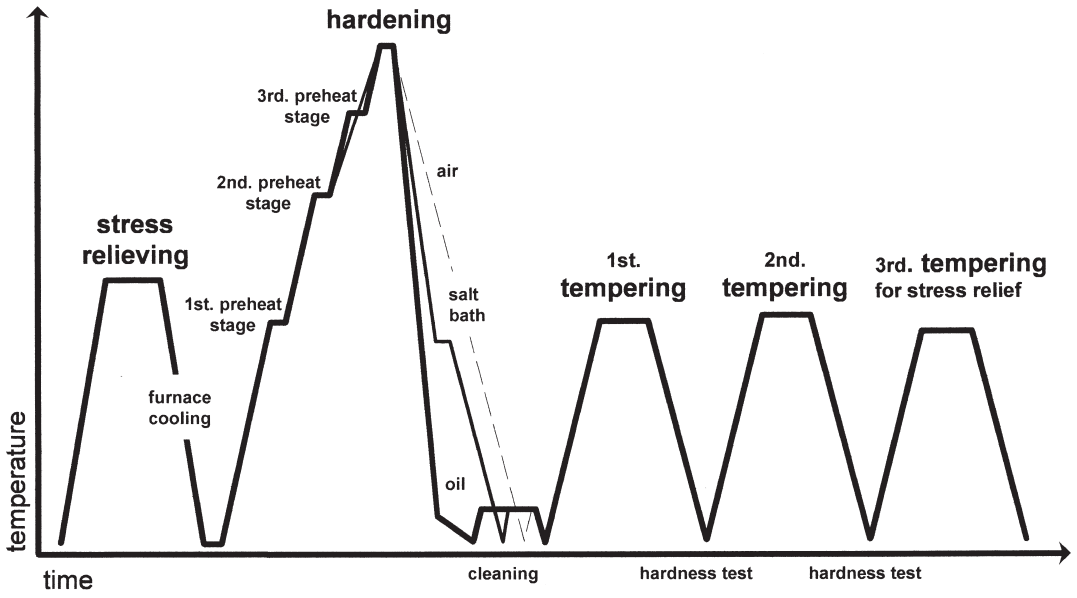

FIG. 6. Heat treatment sequence of high-speed steels.

regularly distributed dark spots (or small areas) of diameters between 3 and 10 nanometers. On the left of Fig. 8 there are vertically oriented elongated line structures (possibly resulting from plate-shaped areas in perpendicular orientation to the specimen surface) of only 2–3nm in thickness. As will be shown by the chemical analysis

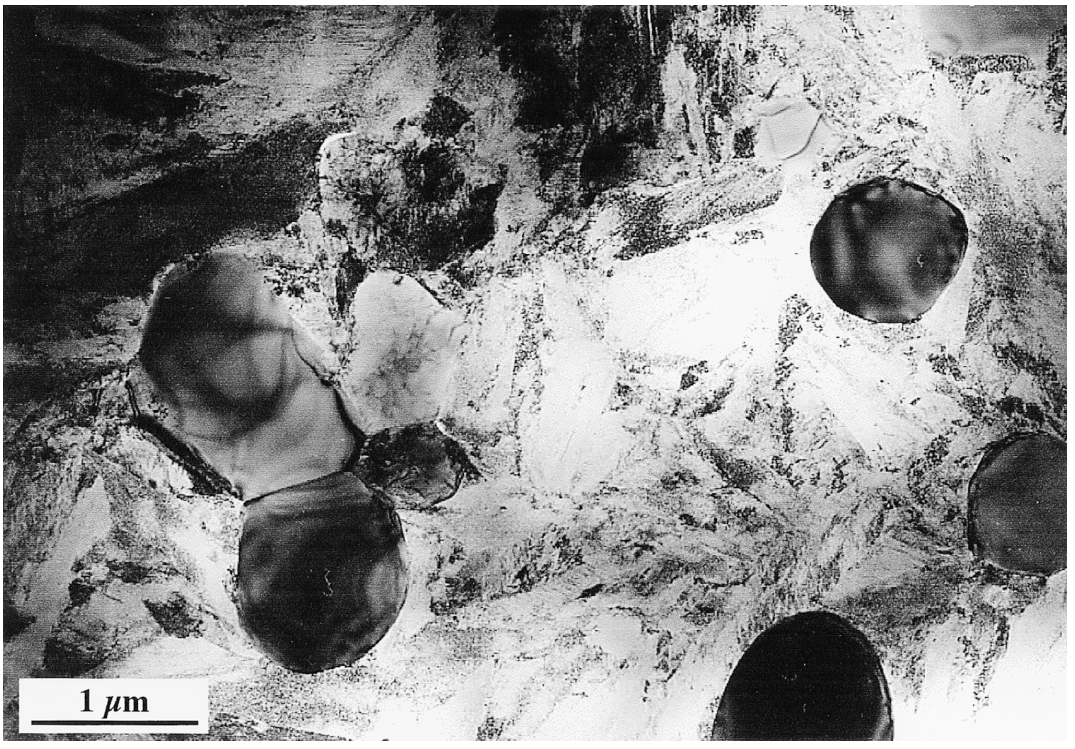

FIG. 7. Microstructure of steel after hardening and tempering (HVEM).

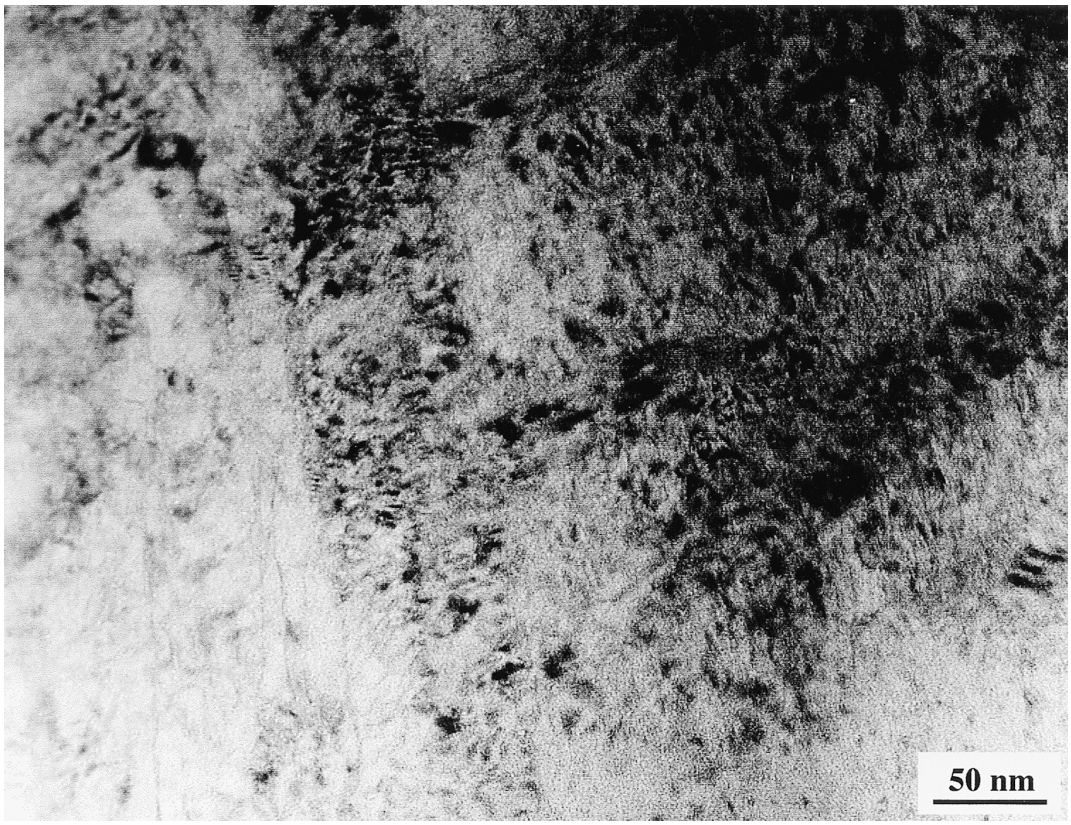

FIG. 8. Strain contrast of secondary carbides.

in our Results section, both these features exhibit a strain contrast of secondary vanadium carbide precipitates. Possibly, the latter have formed in regions of the material where the vanadium concentration is high.

Even for the highest possible resolution (see Fig. 9), the course of the lattice planes does not indicate any irregularities or other phases within the dark areas. There is also no indication of misfit dislocations, which would be typical of the accommodation of lattices of different effective lattice parameters. Hence, the precipitates are supposed to be completely coherent. The same also holds for the thin line-shaped structures. (The disturbances of the lattice planes in Fig. 9 are mainly caused by the preparation-induced surface roughness.)

The finely dispersed precipitates having only a very small misfit to the matrix contribute to the secondary hardening at elevated temperatures [1].

CHEMISTRY AND STRUCTURE OF SECONDARY CARBIDE PRECIPITATES

EFTEM ANALYSIS

The chemical composition and the lateral distribution of the small nanometer-sized carbide precipitates cannot be imaged sufficiently well by the method of X-ray microanalysis: The spatial resolution, on the one hand, is limited by the fluorescence phenomena in adjoining matrix areas. On the other hand, the recording of appropriate X-ray maps take too much time. Therefore, the carbides were analyzed and imaged by the electron energy filter technique (EFTEM) yielding a two-dimensional element distribution.

This new favorable method in materials science is based on the spectroscopy of inelastically scattered electrons (EELS): first, an energy window ($\Delta E = 10 \ldots 30$eV) is in-

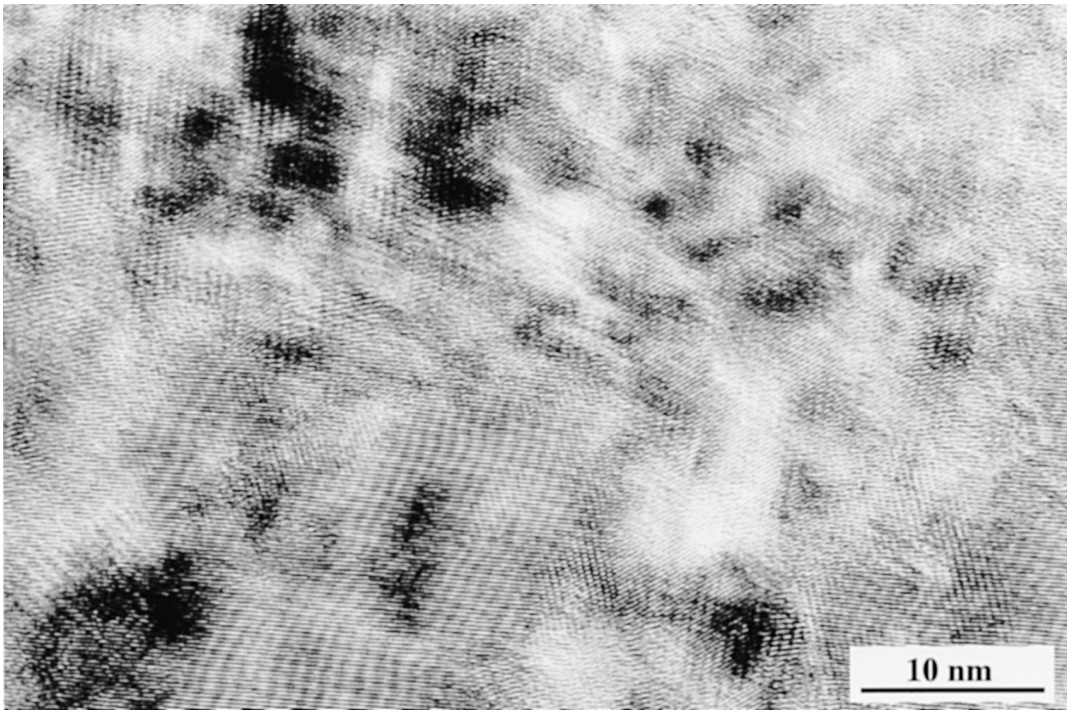

FIG. 9. HREM image of secondary carbides in steel.

serted in the Gatan imaging filter (GIF) behind the characteristic energy loss edge of interest in the EEL spectrum. With the selected electrons, a subsequent electron-optical system forms an image, which is digitized by a slow scan CCD camera. Because of the low specific signal in the EEL spectrum, the background has to be removed by recording one or two additional images using the same energy window in positions directly in front of the edge onset. The calculation of an element specific image is now possible by dividing the image behind the ionization edge by one image in front of it (ratio map), or by subtracting the background, modelled with the two pre-edge images based on an exponential law, from the post-edge image (elemental map). While the latter method results in a true element distribution the former leads to an improved signal-to-noise ratio and is only little affected by varying specimen thickness and diffraction contrast [18]. Qualitatively, both methods should yield similar results, however.

RESULTS

Because of the low energy loss intensity obtained from the extremely small precipitates we first employed the ratio map technique using the low energy region (M-edges) of the EEL spectrum. The positions of the respective energy windows ($\Delta E = 10eV$) in

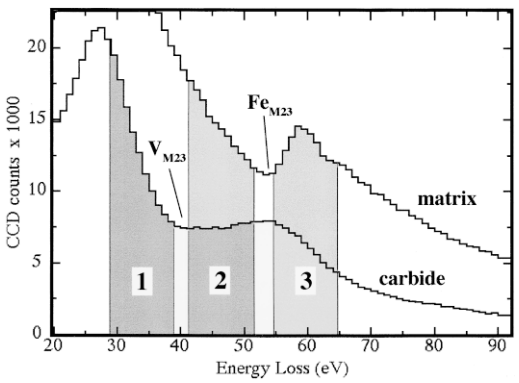

FIG. 10. Position of the energy windows in the EEL spectrum for recording the pre- and post-edge images.

the spectrum are given in Fig. 10. For imaging the matrix (iron, M_{23}-edge onset at 54eV), windows No.3 (post-edge, at 60eV) and No.2 (pre-edge, at 47eV) were used. As it is assumed that the coherent secondary precipitates mostly contain vanadium [19] (V-M_{23}-edge onset at 38eV), windows No.2 (post-edge) and No.1 (pre-edge, at 34eV) were used to detect the carbides. Unfortunately, however, a certain chromium content in the carbide cannot be excluded as the Cr-M_{23}-edge at 42eV overlaps with that of V in window No.2.

As an example, Fig. 11 shows EFTEM images of the typical distribution and composition of nanometer-sized carbides. Most of the dark structures in the TEM bright-field image (a) (see Fig. 8) appear in bright con-

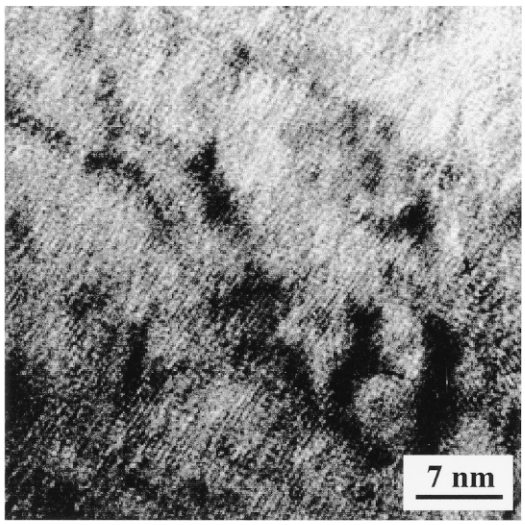

a)

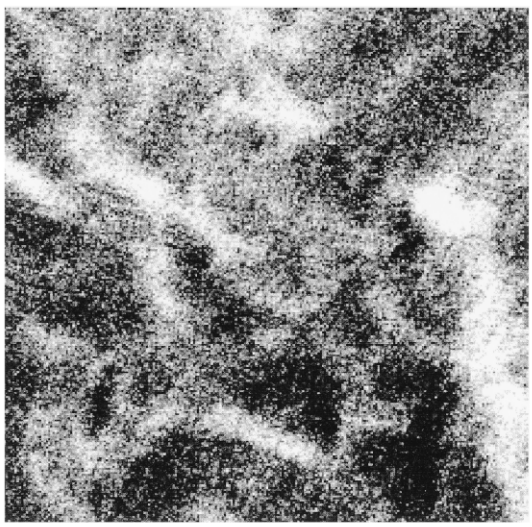

b)

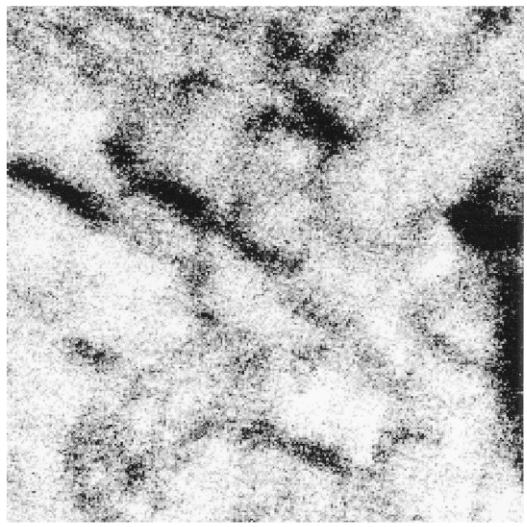

c)

FIG. 11. Nanometer-sized carbide precipitates: (a) TEM bright field, (b) and (c) EFTEM ratio maps of V and Fe, respectively.

trast in the V ratio map (b), i.e., they are rich in this element. Contrary to that, in the Fe ratio map (c) corresponding areas appear dark, i.e., there is no iron, and both images complement each other. It can be concluded that in the investigated steel most of the secondary carbides appear as adjoining precipitates (rods or plates) having a length of 10 nm and a width of only 2nm. Remarkably, it turns out that few dark structures in the TEM bright-field image of Fig. 11a (for example, the parallel stripes in the lower right) do not correspond to carbides. They are rather caused by simple diffraction contrast. Besides, the latter results demonstrate that in materials research EFTEM is a powerful tool of characterizing the nature of smallest TEM contrast phenomena.

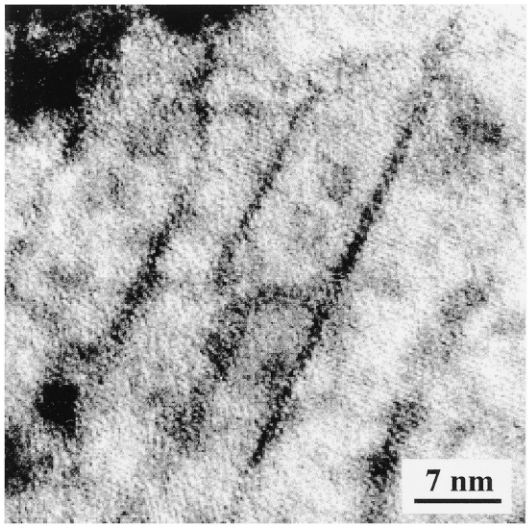

a)

b)

c)

FIG. 12. Rod-shaped carbide precipitates: (a) TEM bright-field, (b) and (c) EFTEM ratio maps of V and Fe, respectively.

Similarly, the more extended line-(plate-) shaped precipitates (see Fig. 8, lower part) are characterized. Figure 12 shows an example of these structures 1–2-nm wide, but some 10 nanometres long. Again, the element specific ratio maps of V (b) and Fe (c) complement each other.

To prove the elongated precipitates to be mainly composed of vanadium and carbon, 3-window elemental maps were additionally achieved. Figure 13 shows that carbon (K-edge at 282eV) (c) occurs in the same places where also vanadium (c) appears but not iron (b). It should be noted that in Fig. 13, the elemental maps are recorded with the V-L_{23}-edge at 513 eV and the Fe-L_{23}-edge at 708 eV. In this energy range, the intensity of the EEL spectrum is usually small, the im-

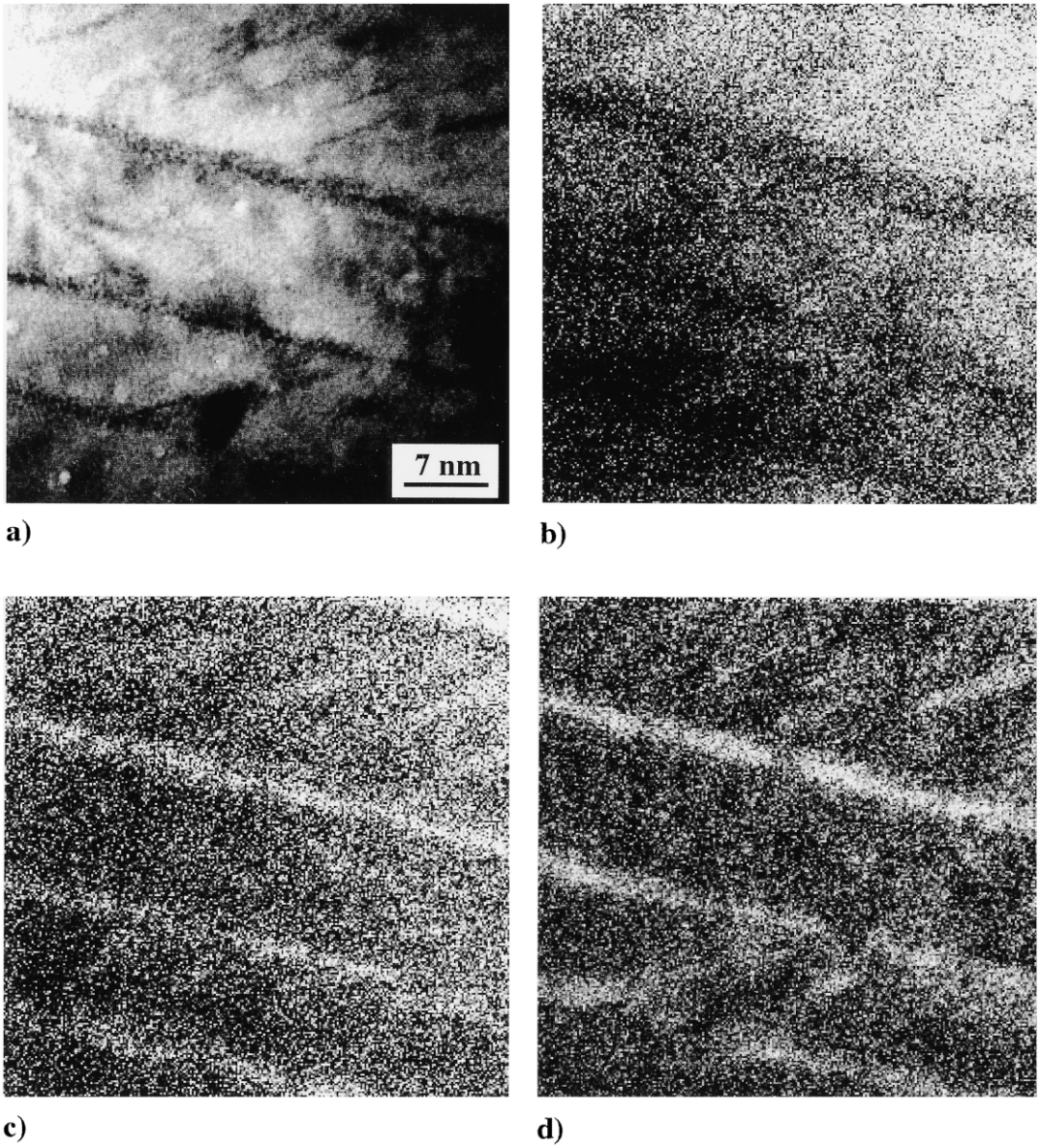

FIG. 13 Rod-shaped carbide precipitates: (a) TEM bright-field, (b), (c), and (d) EFTEM 3 window elemental maps of Fe, V, and C, respectively.

ages become noisy, and nanometre structures will not be resolved. Moreover, in this energy range there is no overlap between V and Cr as in the case of M-edges, i.e., the precipitates definitely contain V and C.

The observed high vanadium content of both types of secondary precipitates suggests them to be carbides of the MC-type [19].

SUMMARY

The production of high-speed steels starts in an electric arc furnace and includes hot forming, annealing, machining, and heat treatment until the tool is accomplished. The material undergoes a number of mechanical and thermal treatments, which influence its macroscopic shape as well as its microscopic structure.

The microstructure was characterized down to atomic dimensions by high voltage (HVEM) and high resolution electron microscopy (HREM) including energy-filtered transmission electron microscopy (EFTEM) for nanochemical analyses. Primary carbides forming during solidification and assuming a more spherical morphology during hot forming, show an incoherent interface to the matrix.

The primary carbides and their distribution have a major influence on the wear resistance and the toughness of the material. During soft annealing in the high-speed steels, additionally annealing carbides 50–300nm in size have precipitated in a ferritic matrix.

After hardening and during tempering, secondary carbides grow, revealing different morphologies. In some regions they appear as regularly distributed dark spots 3–10 nanometers in diameter. In others, rods or plates occur 2–3nm in thickness. HREM investigations revealed a coherent transition to the matrix.

Elemental maps on a nanometer scale were achieved by EFTEM, showing an enrichment with vanadium and carbon and a depletion of iron in the namometer-sized MC-type carbides.

The knowledge of the microstructure of the different phases and their interfaces is needed for micromechanical finite element (FEM) calculations of the structure-property relations. These calculations shall give hints for improving the production route and a better understanding of its effects.

References

1. *Werkstoffkunde Stahl*, Verein Deutscher Eisenhüttenleute, ed., Verlag Stahleisen, Düsseldorf, Germany (1984).
2. S. Karagöz and H. F. Fischmeister: *The Relative Contribution of Primary Carbides and Secondary Hardening to the Performance of high-speed steels*. Proc. 1st Int. High-Speed Steel Conf., pp. 41–51, Leoben (1990).
3. E. Haberling and I. Schruff: Zussammenstellung der eigenschaften und wekstoffkennigrößen des schnellarbeitsstahles S 6-5-2 (Thyrapid 3343). *Thyssen Edelstahl Technische Berichte* 11:99–109 (1985).
4. R. Riedl, S. Karagöz, F. Jeglitsch, and H. F. Fischmeister: Zur Entwicklung der Schnellarbeitsstähle, *Berg- und Hüttenmännisches Monatsheft*, Leoben, 119. Jahrgang, Heft 3, pp. 71–85 (1984).
5. G. Wahl: *Heat Treatment of High Speed Steel Tools in Vacuum Furnaces with Gas Quenching*. Proc. 1st Int. High Speed Steel Conf., pp. 193–200, Leoben (1990).
6. B. Edenhofer, F. Bless, W. Peter, and J. W. Bouwman: *The Evolution of Gas Quenching in Todays Heat Treatment Industry*. Proc. 11th Congress of the Int. Fed. for Heat Treatment and Surface Engineering & 4th ASM Heat Treatment and Surface Engineering Conf. in Europe, pp. 151–161 Florence (1998).
7. T. D. Atterbury: *Heat Treatment of High speed Steels, Vacuum Techniques*. Proc. 1st Int. High Speed Steel Conf., pp. 239–250, Leoben (1990).
8. A. F. Plankensteiner, H. J. Böhm, F. G. Rammerstorfer, V. A. Buryachenko, and G. Hackl: Modelling of layer-structured high-speed steel. *Acta Mater*. 45(5):1875–1887 (1997).
9. A. F. Plankensteiner, H. J. Böhm, F. G. Rammerstorfer, and V. A. Buryachenko: Hierarchical modelling of the mechanical behaviour of high-speed steels as layer-structured particulate MMC's. *J. de Physique* IV(C6):395–402 (1996).
10. O. L. Krivanek, A. J. Grubbens, N. Dellby, and C. E. Meyer: Design and first applications of a post-column imaging filter. *Micr. Microanal. Microstruct*. 3:187–199 (1992).
11. A.-M. Elrakayby and B. Mills: Identification of carbides in high-speed steels. *J. Mat. Sci. Lett*. 5:332–334 (1986).
12. H. Fredriksson and S. Brising: The formation of carbides during solidification of high-speed steels. *Scand. J. Metallurgy* 5:268–275 (1967).

13. J. McLaughlin, R. W. Kraft, and J. E. Goldstein: Characterization of the solidification structures within the dendritic core of M2 high-speed steels. *Metallurgical Transactions* 8A:1787–1792 (1977).
14. H. Brandis, E. Haberling, R. Ortmann, and H. Weigand: Einfluß des siliciumgehaltes auf gefügeausbildung und eigenschaften eines schnellarbeitsstahles mit 6% W, 5% Mo, 2% V, 4% Cr und 1% bzw. 1.5% C. *Thyssen Edelstahl Technische Berichte*, 3:81–99 (1977).
15. H. Fredriksson and M. Nica: The influence of vanadium, silicon and carbon on the eutectic reactions in M2 high-speed steels. *Scand. J. Metallurgy* 8:243–253 (1979).
16. G. Lichtenegger, F. Jeglitsch, G. Pöckl, and G. Hackl: *Carbides in high-speed steels—Aspect of alloy development*. Proc. of the 4th Int. Conf. on Tooling, Bochum, pp. 17–26 (1996).
17. H. Fredriksson, M. Hillert, and N. Nica: The decomposition of the M_2C carbide in high speed steel. *Scand. J. Metallurgy* 8:115–122 (1979).
18. F. Hofer, P. Warbichler, and W. Grogger: Imaging of nanometre-sized precipitates in solids by electron spectroscopic imaging. *Ultramicroscopy* 59:15–31 (1995).
19. J. Janovec, B. Richarz, and H. J. Grabke: Phase transformations and microstructural changes in 12% Cr steel during tempering at 1053 K. *Steel Research* 65:438–443 (1994).

Received August 1998; accepted January 1999.